

LASER INTERFEROMETER GRAVITATIONAL WAVE OBSERVATORY  
- LIGO -  
CALIFORNIA INSTITUTE OF TECHNOLOGY  
MASSACHUSETTS INSTITUTE OF TECHNOLOGY

Technical Note	LIGO-T080074-00-R	2008/09/26
<b>Automated Noise Characterization for the 40 m LIGO Facility</b>		
W. Max Jones		

*Distribution of this document:*

ISC Group

**California Institute of Technology**  
**LIGO Project, MS 18-34**  
**Pasadena, CA 91125**  
Phone (626) 395-2129  
Fax (626) 304-9834  
E-mail: info@ligo.caltech.edu

**Massachusetts Institute of Technology**  
**LIGO Project, Room NW22-295**  
**Cambridge, MA 02139**  
Phone (617) 253-4824  
Fax (617) 253-7014  
E-mail: info@ligo.mit.edu

**LIGO Hanford Observatory**  
**Route 10, Mile Marker 2**  
**Richland, WA 99352**  
Phone (509) 372-8106  
Fax (509) 372-8137  
E-mail: info@ligo.caltech.edu

**LIGO Livingston Observatory**  
**19100 LIGO Lane**  
**Livingston, LA 70754**  
Phone (225) 686-3100  
Fax (225) 686-7189  
E-mail: info@ligo.caltech.edu

<http://www.ligo.caltech.edu/>

## 1 Abstract

The Laser Interferometer Gravitational Observatory (LIGO) is currently prototyping new technologies at the 40 m test bed facility at the California Institute of Technology. Because LIGO's success depends critically on its ability to limit noise sources which may interfere with the detection of weakly interacting gravitational waves, much time and effort has been spent on cataloguing various noise sources. This SURF represents an extension of that effort. A suite of matlab scripts has been developed to automatically compile such a noise catalogue, called a noise budget, for the LIGO sites in Livingston, Louisiana and Hanford, Washington. Efforts have been made in the past to adapt these methods for the 40 m site.

The SURF focused on re-writing parts of the automated noise budget suite to make them compatible with the 40 m facility. Efforts focused on the seismic, DARM, PRC, SRC, and MICH noise sources. Furthermore, a magnetometer was installed at the 40 m site to measure the effect of nearly static magnetic fields on the beam splitter optic.

## 2 Overview of LIGO

General relativity predicts that rapid changes in a local gravitational field will propagate outward at the speed of light as gravitational waves. Gravitational waves take the form of plane waves in space time which interact with matter by stretching space-time along one axis while simultaneously compressing space-time along a perpendicular axis. Due of the relative weakness of the gravitational force, gravitational waves do not interact strongly with matter. This fact presents the ambitious observer with a unique opportunity. Because of the weak coupling, only very large masses moving rapidly will produce gravitational waves of significant size. Among these types of sources are inspiraling black holes, inspiraling neutron stars, and pre-recombination inflation. Furthermore, the weak coupling of gravitational waves to matter means that unlike electromagnetic waves, gravitational waves will not be significantly absorbed or scattered by matter between the source and the observer. This signifies that an observer who can construct a device to measure the infinitesimal effects of a passing gravitational wave will have a direct observational window to some of the most interesting and least understood phenomena in our universe.

The Laser Interferometer Gravitational Wave Observatory (LIGO) project is a joint venture between the Massachusetts Institute of Technology (MIT) and the California Institute of Technology (Caltech) to design, develop, construct, and operate devices capable of detecting gravitational waves. To this end LIGO has constructed three interferometers: a 4 km arm-length interferometer in Livingston, Louisiana and two interferometers in Hanford, Washington with arm-lengths of 2 km and 4 km respectively. A Michelson interferometer in its most basic form consist of a laser, a beamsplitter, two mirrors, and a photodetector. A laser beam is directed to the beamsplitter. A fraction of the incident beam passes through the beam splitter to continue down the x-arm of the interferometer to the x-arm end test mass mirror (ETMX). There the light is reflected directly back along its incoming path to the beam splitter. Simultaneously, the non-transmitted incident laser light is reflected along the orthogonal y-arm of the interferometer to an identical end test mass mirror ETMY that again reflects the beam directly back to the beam splitter. A fraction of each of the reflected

beams will interfere at the anti-symmetric port and produce an interference fringe pattern on the photodetector. By carefully manipulating the optical lengths of both arms an operator can create total destructive interference at the anti-symmetric port. This is the manner that the LIGO interferometers are operated in. A passing gravitational wave will lengthen the arms differentially, disturbing the state of destructive interference in a manner that allows one to determine the change in absolute arm-length difference,  $\Delta l = |l_{x\text{-arm}} - l_{y\text{-arm}}|$ .

The best predictions indicate that passing gravitational waves of interest to LIGO may induce a strain of amplitude as small as  $10^{-21}$  in the frequency range 40-7000 Hz [9]. With arm-lengths on the order of 1 km this implies that to detect the presence of such waves LIGO interferometers must be able to register a change in differential arm-length on the order of  $10^{-18}$  m. *This is one-thousand times smaller than the diameter of a proton.* A traditional interferometer set-up would be incapable of measuring such infinitesimal changes.

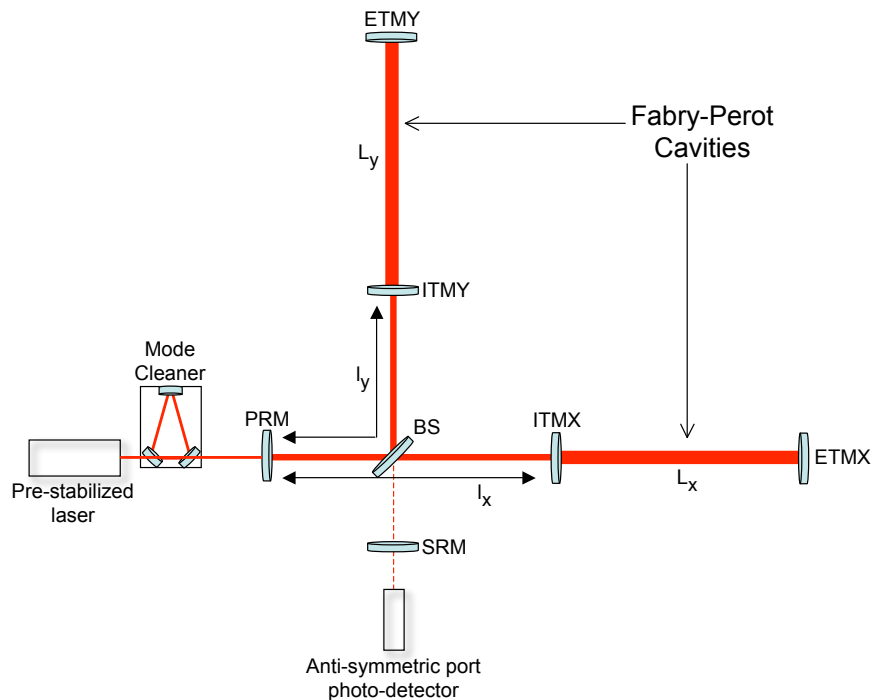


Figure 1: Interferometer Layout

To achieve these sensitivities LIGO implements several novel subsystems. For example, by placing input test mass mirrors in each arm with mirrored sides facing away from the input beam each arm is turned into a Fabry-Perot cavity. Light in each arm becomes trapped in the Fabry-Perot cavity which is created by keeping each ITM/ETM pair an integer number of wavelengths apart. The resulting signal power amplification produces a proportional increase in sensitivity. Two more power amplifying optical cavities are also created by placing a power-recycling mirror (PRM) before the beam splitter in the input light path and by placing a signal-recycling mirror (SRM) before the anti-symmetric port photo-detector. The upside is that the power amplification resulting from these cavities allows the photo-detector to detect the subtle change in the anti-symmetric port signal that would result from a passing gravitational wave. The downside is that each of the cavities must be kept in resonance

(the distance between the optics in the cavities must be an integer number of wavelengths). A complex array of control loops and actuators serve to keep the cavities in resonance by adjusting the optic position to cancel any disturbance, gravitational or otherwise. This implies that during normal operation no signal will be detected at the anti-symmetric port and any signal resulting from a passing gravitational wave will have to be extrapolated from the control signals sent to each optic.

Since the presence of any disturbance must be detected via the resonance control loops, it is necessary to distinguish gravitational wave signals from those due to non-gravitational source. While careful data analysis of the control channels makes it unlikely that LIGO researchers would misinterpret a gravitational wave for some other type of disturbance, the extremely weak nature of an incoming gravitational wave means that it is entirely possible that other disturbances will "wash out" the desired signal. For example, seismic activity at the interferometer site could cause optic movement orders of magnitude larger than the apparent optic movement caused by a gravitational wave. Frequency noise in the incoming laser light could net the same effect since slightly different frequencies of light would not all interfere with complete destruction at the beam splitter and thus would register as a single at the anti-symmetric port photo-detector. This noise signal would propagate to a control correction.

### 3 Overview of LIGO Noise Budget

From the last paragraph in the previous section, it may be apparent that an enormous amount of LIGO's efforts are concentrated in the area of noise source identification and reduction. It is in this area that this research paper is concentrated. A *noise budget* is a comprehensive catalogue of important noise sources as well as their effect on the gravitational wave signal channel, in this case C1:LSC-DARM\_ERR. The goal of this project was to create an accurate noise budget for the 40 m test bed facility here at Caltech.

The sample noise budget in figure 2 shows a a noise budget for the 4 km interferometer at Hanford, Washington. The green dashed line indicates the total noise in the DARM channel as the sum of the noise from different sources. The units on the y-axis are those of  $m/\sqrt{(Hz)}$ . That is to say, if  $S(\omega)$  is the total noise, the absolute uncertainty in arm length at frequency  $\omega$  is given by

$$\sqrt{\omega S(\omega)^2}$$

with units of meters.

To measure the impact of a particular source upon the C1:LSC-DARM\_ERR channel one must place sensors to measure the disturbance at its source. For example, seismic motion will be translated into optic motion which will directly alter the DARM signal. To measure seismic motion, one would place accelerometers near the optics. One assumes that the source noise is linear: the noise source is related to the C1:LSC-DARM\_ERR by the relation

$$O(\omega) = I(\omega) * T(\omega)$$

where  $O(\omega)$  and  $I(\omega)$  are the output noise and input noise respectively as a function of frequency  $\omega$ .  $T(\omega)$  is the transfer function which must be measured experimentally or cal-

H1: UGF = 206 Hz, 15.3 Mpc, Predicted: 17.1, Apr 06 2007 12:23:54 UTC

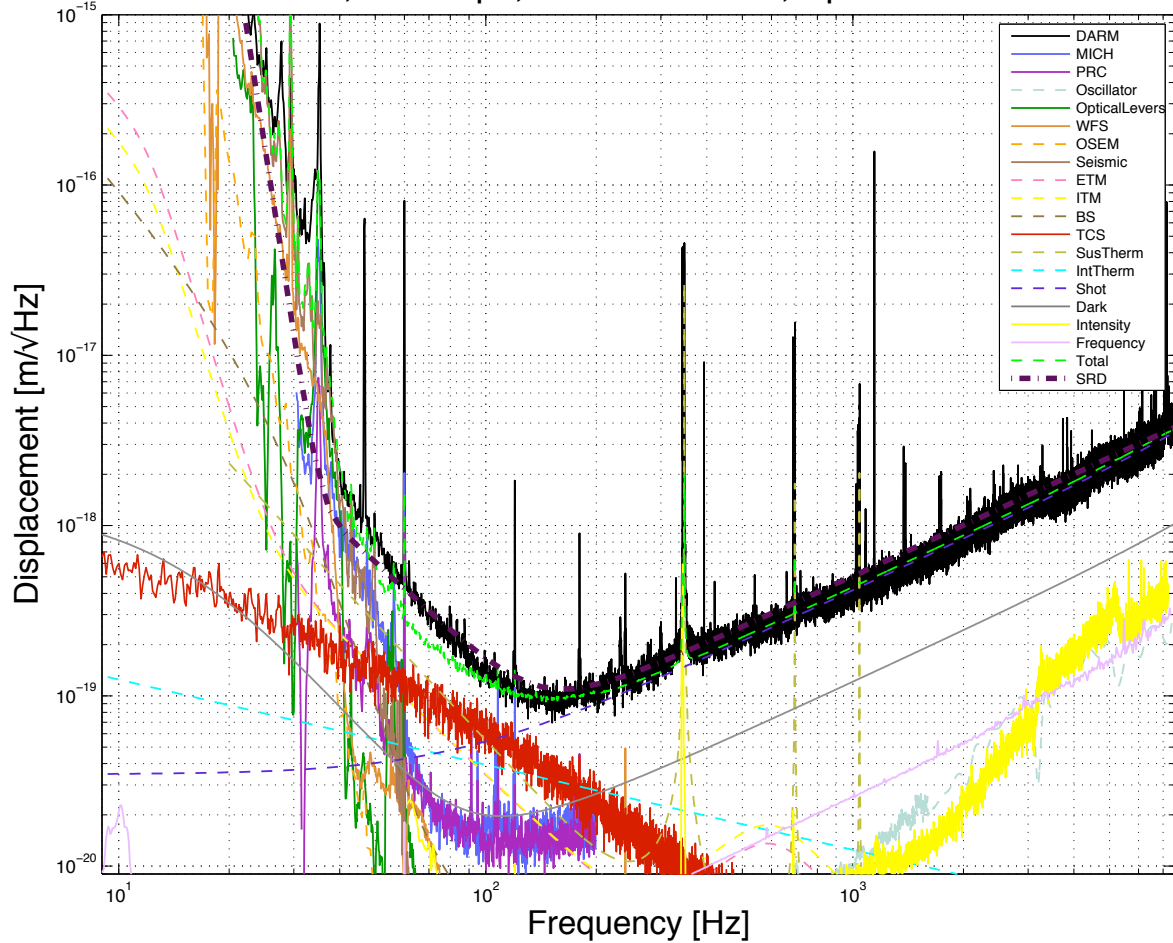


Figure 2: A noise budget for the 4 km LIGO interferometer in Hanford, Washington.

culated theoretically for each noise source. In the seismic case, the transfer function was theoretically generated as the product of multiple transfer functions.

Previous work to construct a noise budget for the 40 m facility has centered around modifying existing methods for creating an automated noise budget. The sites at Livingston, Louisiana and at Hanford, Washington both use a set of MATLAB scripts to regularly create noise budgets. The goal is to modify that code to work at the 40 m site. These modifications are non-trivial since new transfer functions must be measured for each noise source and new sources specific to the 40 m site must also be added to the scripts while preserving cross-site functionality. Previous SURF students [5] [10] measured the transfer for the seismic noise source and added it to the working noise budget. I intended to build on their work by adding and correcting as many noise sources as possible to the noise budget catalogue.

The sources investigated in detail in this paper are the following: seismic, thermal, displacement, and output electronics noise. Remaining sources which were not investigated in sufficient detail for this project include dark noise, shot noise, laser intensity noise, laser frequency noise and magnetic noise.

My time at the 40 m facility was spent learning the fundamentals of laser interferometry, understanding LIGO's noise budget protocol, as well as two brief side projects (calibrating a Bartington magnetometer and helping to clean a set of baffles to be installed at the 4 km sites a Livingston, Louisiana and Hanford, Washington). The results of my research include a noise budget program modified to successfully run at the 40 m facility and a calibrated and installed magnetometer.

## 4 Noise Budget Development

A block diagram of the current noise budget script is shown below. The procedure begins with the activation of `getNoiseBudget.m` which together with `runmeas.m` sets file paths specific to each site and calls the script `NoiseBudget.m`. `NoiseBudget.m` updates the pre-loaded parameter files with `updatepardata.m`. Then `NoiseBudget.m` calculates the unitary gain frequency with `getUGF.m` and takes data from each of the source channels with files such as `getSeismic.m`. The `get` files take data and with a known transfer function calculates the noise contribution. `NoiseBudget.m` then plots and saves the noise budget.

### 4.1 Thermal Noise

LIGO's optics are suspended by piano wire in a vacuum chamber which is held a room temperature. In this state, one important concern is that internal thermal vibrations in the mirror or its suspension wire will be coupled to the DARM measurement. The dielectric surface of the cavity mirrors cause a non-negligible loss of laser light to thermal motion [13]. Furthermore, while the mirror has no significant resonances in the measured axis and range, the suspension wire has high Q-factor violin modes between 100-1000 Hz. These modes are clearly visible in the Hanford and 40 m noise budgets.

#### 4.1.1 Calculation of Thermal Noise

The noise budget script employs the functions `getIntTherm.m` and `mirror_thermal.m` to calculate the contribution of the internal thermal noise of the mirrors to DARM noise. The calculation is completely theoretical and relies on the work of Andri Gretarsson [3] to calculate the spectral noise density.

The `noisebudget` script employs the functions `getSusTherm.m` and `PendThermTE.m` to calculate the contribution of suspension thermal noise to the DARM noise. The calculation is also completely theoretical and relies on the work of Gabriela Gonzalez [4] to calculate the spectral noise density.

#### 4.1.2 State of Thermal Noise Protocol

The `mirror_thermal.m` uses several hard-coded constants to calculate the DARM noise due to internal thermal vibrations of the mirror. These constants should be reviewed and, if necessary, should be altered with a case statement to reflect 40 m parameters. Otherwise,

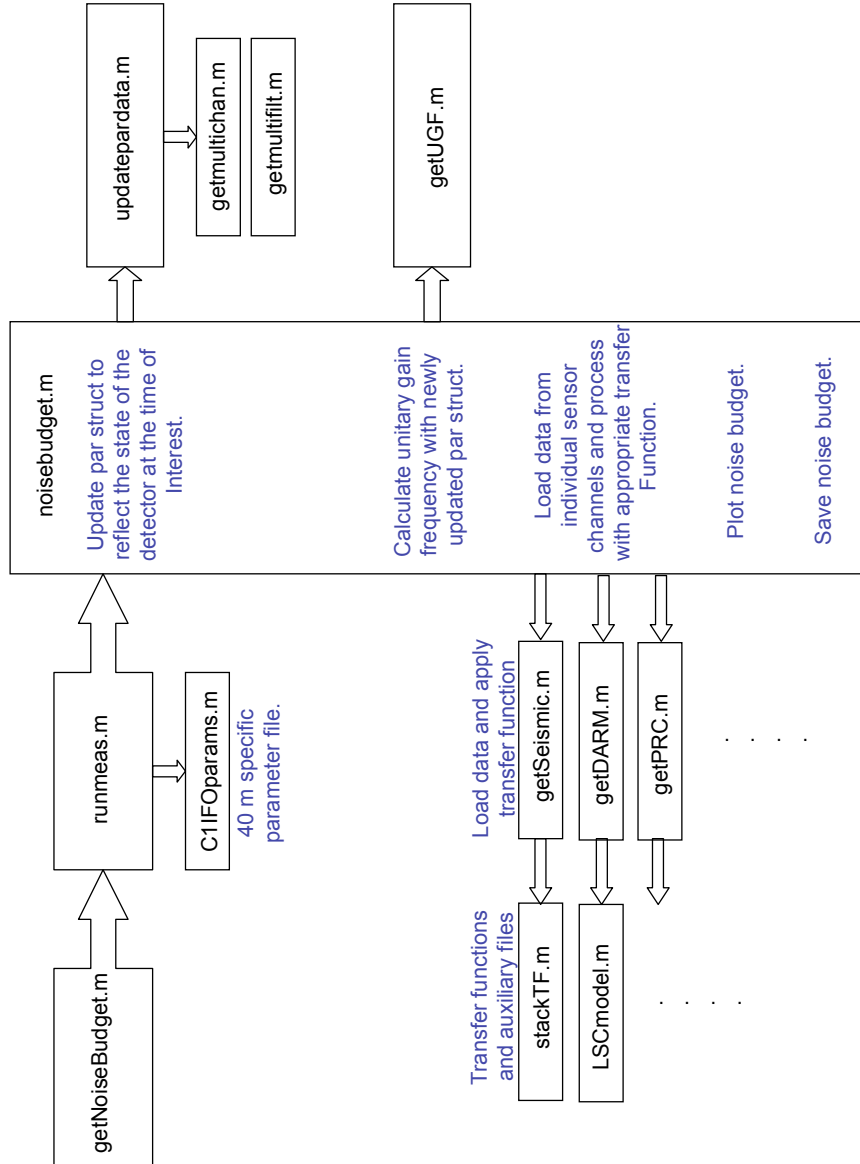


Figure 3: Noise Budget Script Block Diagram

the thermal noise protocols appear to get reasonable results as seen by comparing suspension thermal noise and internal thermal noise between Fig. 2 and Fig. 5.

## 4.2 Seismic Noise

Among the primary gravitational wave sources LIGO hopes to detect are inspiraling neutron stars (or black holes) and primordial gravitational wave background. It is thought that inspirals will emit gravitational waves in the range of a few hundred hertz or lower for a brief period of time before coalescence and furthermore that the gravitational background may be on the order of a 100 hertz. [12]. Therefore, it is extremely important for LIGO to achieve maximum sensitivity in this frequency band.

At frequencies lower than 100 hertz, the main source of noise is seismic motion at the sites. Ground motion is translated into a change of the arm cavity optical length which is translated to signal at the dark port.

To attenuate optical motion due to seismic activity, all major optics are suspended from pendulums. These pendulums are in turn bolted to the top of a series of four spring and plate passive seismic isolators. The spring and plate system is referred to as the seismic isolation stack. The pendulum is designed to have a resonant frequency of .75 hertz [13], well below the frequencies which LIGO expects to be able to detect gravitational waves. The same is true for each of the spring/mass systems comprising the stack. Far from resonance, these elements are approximately simple harmonic oscillators and so the frequency dependent amplitude of their oscillations  $A(\omega) \propto \omega^{-2}$ . Therefore the total transduced amplitude  $A_{total}$  is the product of the amplitude attenuations of the simple states,  $A_{total} \propto \omega^{-8}$  [14].

#### 4.2.1 Seismic Noise Calculation

As explained above, the noise budget script employs the the function `getSeismic.m` to calculate the contribution of seismic sources to noise in the DARM signal. Two 3-axis Wilcoxon 731A accelerometers are located near the arms with x- and y-axis accelerometers parallel to the ground. The accelerometers are connected to control room computers which read each channel in a dimensionless unit counts. The function `getSeismic.m` samples these channels for a given period of time, converting counts to acceleration using the following formulation [11]:

$$\frac{4 \text{ volt}}{16 \text{ bit resolution}} = \frac{4 \text{ volt}}{2^{16} \text{ bits}} = 61.035 \frac{\mu\text{v}}{\text{count}}$$

The accelerometers transduce acceleration along the axis into output voltage using the following conversion factor

$$\frac{100\text{V}}{9.8 \frac{\text{m}}{\text{s}^2}}$$

so that the total conversion factor is  $5.9824 * 10^{-6} \text{m cts s}^{-2}$ .

The ground is assumed to be a simple harmonic oscillator oscillating at frequency  $\omega$  so that to first approximation the ground displacement amplitude is equal to ground acceleration divided by  $\omega^2$ . Given the ground acceleration, transfer functions modeling the stack and the pendulum are used to convert ground displacement into optical displacement

#### 4.2.2 State of Seismic Noise Protocol

I have rewritten `getSeismic.m` and `SeismicNoise40.m` to be compatible with the current 40 m facility configuration and to be clearer and more easily modified. It may be necessary to remeasure or recompute the stack or pendulum transfer functions.

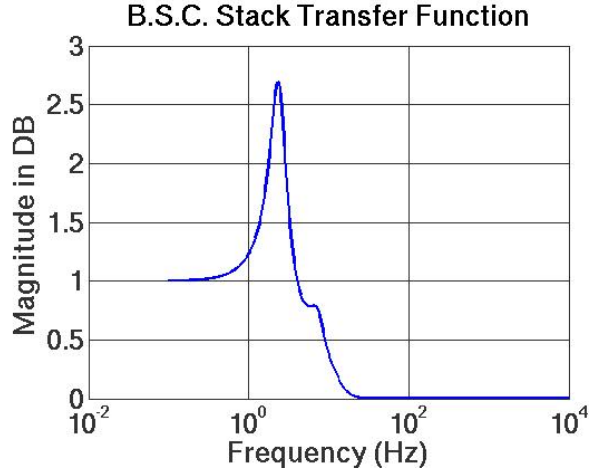


Figure 4: Stack Transfer Function for the Beam Splitter Chamber

### 4.3 Displacement Noise

As stated before, the detection channel C1:LSC-DARM\_ERR measure the differential arm length

$$\Delta(\delta L_d) = \Delta\left(\frac{L_x - L_y}{2}\right)$$

But changes in the lengths of the Michelson, signal recycling mirror, and power recycling mirror cavities may also produce a noise signal at the anti-symmetric port photo-detector. Length changes in the cavities are mostly seismic in origin and the couplings are subtle[13].

#### 4.3.1 Calculation of the Displacement Noise

The noise budget script employs the functions getMICH.m, getPRC.m, and getSRC.m, to calculate the contribution of each cavity's length changes to C1:LSC-DARM\_ERR. Each of these functions employs the ancillary function get\_dtt\_dataset.m to retrieve the OSEM control data for each cavities optics. This data is multiplied by an appropriate, pre-measured transfer function between cavity displacement and DARM signal and also by the open loop gain associated with the DARM control loop provided by LSCmodel.m.

#### 4.3.2 State of Displacement Noise Protocol

I have created the file getSRC.m, since the main sites do not use signal recycling mirrors as yet. It may be necessary to remeasure the transfer functions in C1\_MICHPRC\_TF.mat since this file is a direct copy of the Hanford transfer file H1\_MICHPRC\_TF.mat.

### 4.4 Output Electronics Noise

The OSEM coils located on the initial test masses (ITMs) and end test masses (ETMs) has associated with them a certain amount of electronics noise. The electronics noise is mostly

due to digital to analog signal conversion and the insertion of a de-whitening filter necessary for the coil to meet design specification [13]. Since this noise can result in optic movement, the noise is directly coupled to the channel C1:LSC-DARM\_ERR.

#### 4.4.1 Calculation of Output Electronics Noise

The noise budget script employs the functions getETM.m and getITM.m to calculate the contribution of output electronics noise to the channel C1:LSC-DARM\_ERR. Both these functions employ output\_electronics.m in a theoretical calculation of the desired noise.

#### 4.4.2 State of Output Electronics Noise Protocol

The functions getETM.m and getITM.m needed no initial modification to run at the 40 m facility. Since both functions as well as output\_electronics.m use many hard coded electronics parameters, it may be necessary now or after future upgrades to manually alter these files.

### 4.5 DARM noise

As stated before, the channel C1:LSC-DARM\_ERR represents the change in length difference between the Fabry-Perot cavities in each arm. Changes in the Fabry-Perot cavity length with resonance frequency  $f_c$  should cause signals at the dark port with a gain of

$$-\chi g_{cr} t_{sb} r'_c \frac{1}{1 + i f / f_c} k \delta L$$

where

$$r'_c = \frac{(1 - r_{ITM}^2) r_{ETM}}{(1 - r_{ITM} r_{ETM})^2}$$

where  $\chi$  is a standard pre-factor,  $r_{ITM}$  and  $r_{ETM}$  are the reflectivities of the input and end test masses respectively,  $t_{sb}$  is the sideband frequency transmission coefficient for the cavity, and  $g_{sb}$  is the sideband frequency gain coefficient for the cavity [13].

Under normal operations, this difference is held fixed by automated control loops and furthermore arbitrarily defined to be zero. This is especially true for the 40 m facility since the comparatively short length of the arms implies that the interferometer lacks the ability to actually detect gravitational waves. Therefore, any signal from C1:LSC-DARM\_ERR is considered noise and moreover this noise is a direct measure of LIGO's ability to detect gravitational waves. Models are applied to other noise sources specifically to estimate the affect of each source on this channel. The estimated total predicted noise is then compared to the actual noise in the C1:LSC-DARM\_ERR channel to test the possibility of inaccurate models or unaccounted for noise sources.

## 5 Conclusions

The 40 m facility is a test bed for new technologies that will be implemented at the main sites as part of advanced LIGO. For example, the signal recycling mirrors a part of the Ad-

vanced LIGO program and have been installed at the 40 m facility to test locking feasibility ("locking" is the act of putting all or some of the interferometer cavities into a state of resonance maintained with automatic control loops). This fact makes an accurate noise budget of extreme importance. I would like to acknowledge Rana Adhikara, Alberto Stochino, Rob Ward, the staff of the 40 m facility, LIGO and the Caltech SURF program.

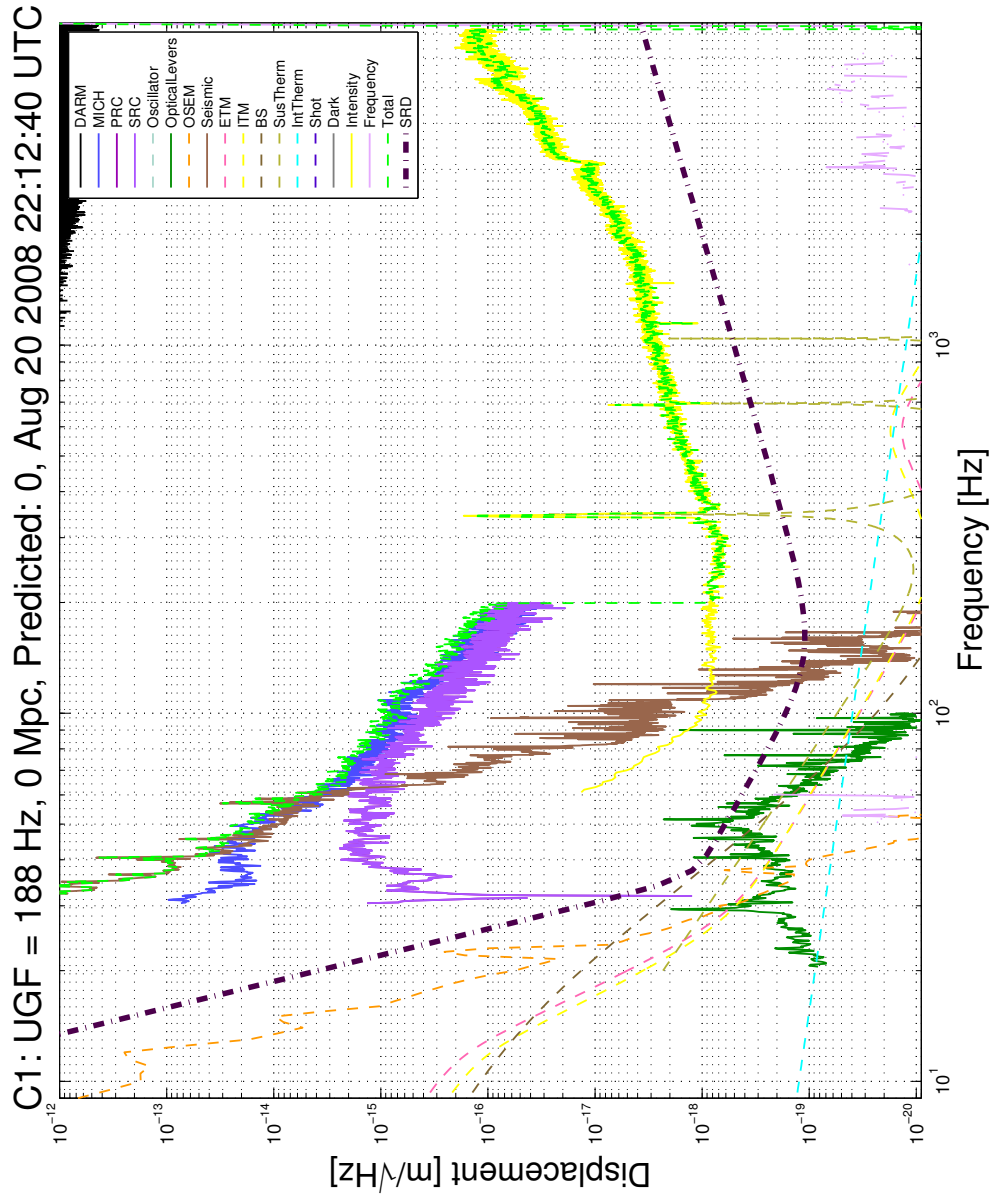


Figure 5: 40 m Noise Budget

## References

- [1] R. Adhikari.
- [2] J. Garofoli.

- [3] Andri Gretarsson.
- [4] Gabriela Gonzalez. "Suspensions thermal noise in the LIGO gravitational wave detector". *Class. Quantum Grav.*, 2000.
- [5] D. Malling. "Development of a Prototype for the LIGO 40 m. Prototype". SURF Paper, California Institute of Technology, 2006.
- [6] Unknown Author. "Shot Noise". [http://en.wikipedia.org/wiki/Shot\\_noise](http://en.wikipedia.org/wiki/Shot_noise).
- [7] Unknown Author. "LIGO". <http://en.wikipedia.org/wiki/LIGO>.
- [8] Unknown Author. "LIGO Fact Sheet". [http://www.ligo.caltech.edu/LIGO\\_web/about/factsheet](http://www.ligo.caltech.edu/LIGO_web/about/factsheet)
- [9] LIGO Science Collaboration. "LIGO: The Laser-Interferometer Gravitational-Wave Observatory". <http://www.arXiv.org>, 2007.
- [10] R. Kinney. "Development of Noise Budget for the LIGO 40m IFO". SURF Paper, 2005.
- [11] R. Kinney. "Noise Budget Development for the 40 Meter Prototype". SURF Presentation, 2005.
- [12] J. Giame et al. "A passive vibration isolation stack for LIGO: Design, modeling, and testing". *Review of Scientific Instruments*, January 1996.
- [13] R. Adhikari. "Sensitivity and Noise Analysis of the 4 km Laser Interferometric Gravitational Wave Antennae" Ph. D Thesis, Massachusetts Institute of Technology, July 2004.
- [14] F. Crawford. *Waves : Berkley Physics Course 3*. unknown copyright.

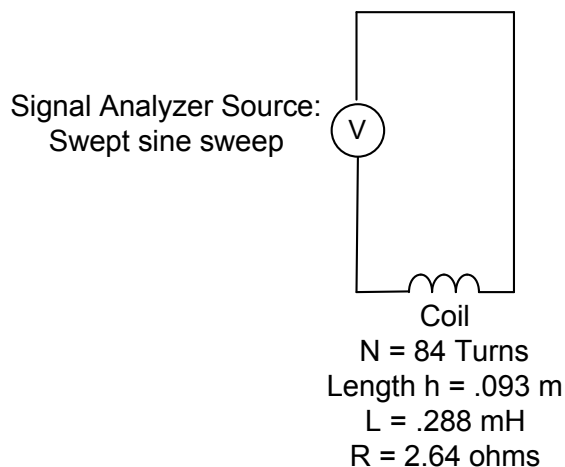
## A Calibration of the LIGO 40m Bartington Magnetometer

### A.1 Overview

The Bartington MAG03MC Three Axis Magnetometer is designed to measure slow changing magnetic fields of strength  $\pm 100\mu\text{T}$  (with 12 volt power supply). The magnetometer is necessary to measure the static magnetic fields around the test masses which are currently an unaccounted for source of noise. Because the magnetometer was purchased in 1992 and has been out of use for several years, it was necessary to calibrate the magnetometer.

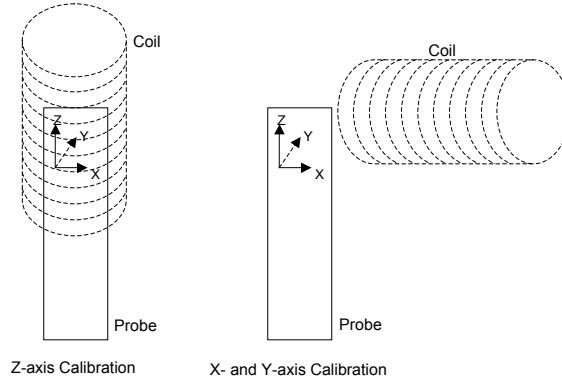
### A.2 Set - Up

To calibrate the three perpendicular axis, two different experimental set-ups were employed. Both set-up s employed the circuit displayed below.



The spectrum analyzer performed a swept sine transfer function measurement by outputting a voltage sine wave of specified amplitude and varying frequencies into the circuit shown above. The resulting oscillating magnetic field produced an oscillating voltage signal from the magnetometer probe. This signal acted as the input for the spectrum analyzer.

To calibrate the z-axis of the magnetometer (the axis parallel with the probe length), the probe was inserted into the middle of the coil such that the z-axis flux-gate magnetometer was at the center of the coil. To calibrate the x- and y-axis flux-gate magnetometers, the coil was moved such that the the the end field of the coil was perpendicular to the axis being calibrated as shown in the figure below.



### A.3 Theory

Let  $V_o$  be the rss (root sum of squares) voltage read at the input channel of the spectrum analyzer. We then assume based on the magnetometer manual that

$$\begin{aligned} V_o &= \alpha B \\ &= \alpha(B_{bk} + B_{coil}) \end{aligned}$$

where  $B_{bk}$  is the background magnetic field and  $B_{coil}$  is the magnetic field resulting from the coil. We know from basic physics courses that if we assume that the coil is sufficiently long in comparison to it's width then the field  $B_{coil}$  is parallel to the direction of the solenoid with the magnitude

$$B_{coil} = \mu_0 \frac{NI}{h}$$

where

$$I = \frac{V}{Z} = \frac{V_i \cos(\omega t)}{Z}$$

where the impedance  $Z$  is given by

$$Z = R + j\omega L$$

so that

$$I = \frac{V_i \cos(\omega t)}{R + j\omega L}$$

By using a spectrum analyzer in swept sine mode we may eliminate the background magnetic field from consideration since only the magnetic field produced by the coil will oscillate with the same frequency as the input voltage. The transfer function  $\frac{V_o}{V_i}$  will be given by

$$\begin{aligned} \frac{V_o}{V_i} &= \alpha B_{coil} \\ &= \mu_0 \frac{\alpha N}{h} \frac{\cos(\omega t)}{R + j\omega L} \end{aligned}$$

Therefore, the magnitude of the transfer function is

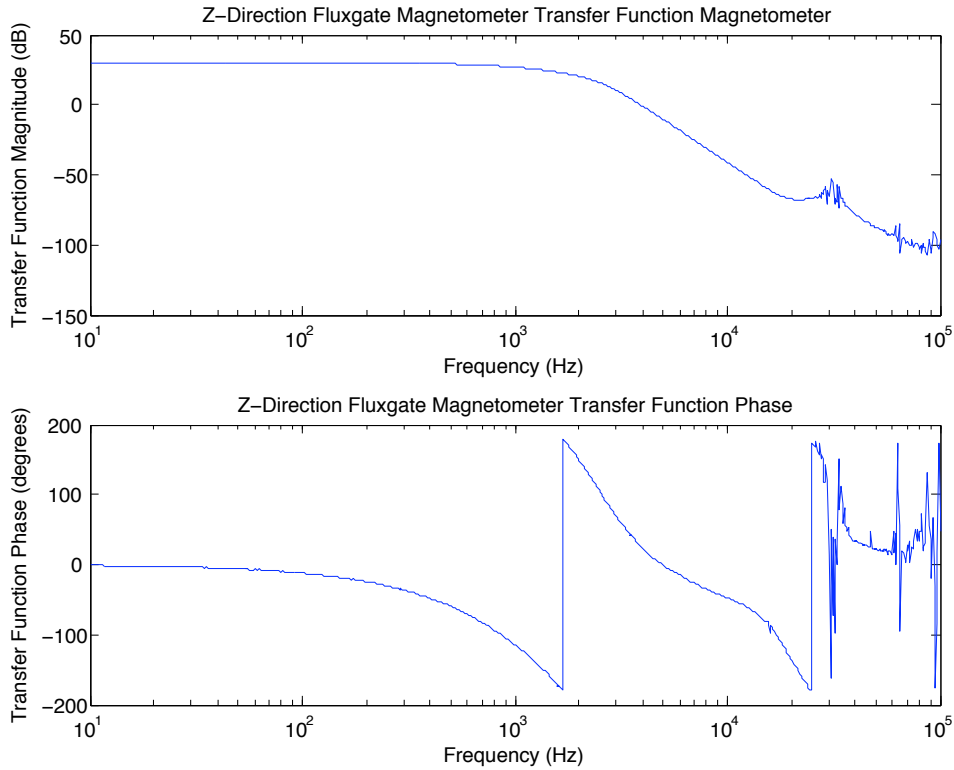
$$\begin{aligned} \left| \frac{V_o}{V_i} \right| &= \mu_o \frac{\alpha N}{h} \frac{\cos(\omega t)}{R^2 + \omega^2 L^2} \\ &\approx \mu_o \frac{\alpha N}{hR} \text{ for } \omega \ll \frac{R}{L} \end{aligned}$$

We may determine that  $\omega$  is sufficiently small by examining the phase of the transfer function. The phase will be nearly zero for small  $\omega$ .

#### A.4 Data

The transfer function for the z-axis magnetometer is shown below. During experimentation it became apparent that fringe affects were dominating the magnetic field measurements necessary in the x- and y-axis calibrations.

We see in the figure that while the phase becomes non-zero above approximately  $10^2$  Hz the magnitude of the transfer function is constant below approximately  $10^3$  Hz.



## A.5 Experimental $\alpha$ value

We use matlab to average the transfer function magnitude for the frequency range 0 -  $10^3$  Hz.

$$C_z = 29.6637 \pm .6876 \text{ dB} = 30.4218 \pm 2.40618$$

From the theory section we are led to believe that

$$\alpha = C_z \frac{hR}{N\mu_0}$$

Therefore

$$\alpha = 14.1324 \frac{\text{nT}}{\text{mV}} \pm 1.12934 \frac{\text{nT}}{\text{mV}}$$

Due to the aforementioned difficulties in measuring the other axis of the magnetometer. We will make the assumption here that  $\alpha$  is constant for all magnetometers.

## B Revised Seismic Code

```

function seismos = getSeismic(par, noise_par, gpstime)

% Author: Unknown
%
% This function calculates the seismic contributions to
% the inteferometer noise budget.
%
% The function must be run from inside NoiseBudget.m to insure
% the necessary definitions exist.
%
% Concerns:
% 1) In the Hanford and Livingston case, the seism and seismv
% are both redefined to exclude the first row (omega = 0). This
% is reasonable since seism and seismv are later divided by omega^2.
% Later, the matrices sent to SeismicNoise.m are seism and seismv
% excluding the first row (now omega = omega_increment). I don't
% see why this should be the case but I've been advised by my
graduate
% student to leave it alone.
%
% Revisions:
% 1) Revised from previous version to incorporate 40m site as well
% as more comments (sorry for the reading). M. Jones 07/25/08.
%

global IFO_NAME FOTON_dir NB_DIR DARM_UGF DATA_dir UTIL_DIR coupldir
...
NDS_HOST NDS_CHANNELS;

disp('Calculating Seismic Noise...')

% Acquiring channel data from get_dtt_dataset.m->get_dtt_FFT.m The
% returned matrices have the following form:
%
% | f | c | c | ... |
% | r | h | h | ... |
% | e | 1 | 2 | ... |
% | q | . | . | ... |
% | . | . | . | ... |
% | . | . | . | ... |
%
% The frequency column is in Hz and the Ch columns are in counts.
switch IFO_NAME
case 'H1'
    disp('Using data from H1')
    seism = get_dtt_dataset('SEISH1', gpstime);
    seisv = get_dtt_dataset('SEISVH1', gpstime);
case 'H2'

```

Figure 6: Revised getSeismic.m Function Page 1

```

    disp('Using data from H2')
    seism = get_dtt_dataset('SEISH2', gpstime);
    seisv = get_dtt_dataset('SEISVH2', gpstime);
case 'L1'
    disp('Using data from L1')
    seism = get_dtt_dataset('SEISL1', gpstime);
    seisv = get_dtt_dataset('SEISVL1', gpstime);
case 'C1'
    disp('Using data from C1')
    seism = get_dtt_dataset('SEISC1', gpstime);
    seisv = get_dtt_dataset('SEISVC1', gpstime);
otherwise
    disp('unknown IFO')
end

% It is necessary to convert the data returned from
get_data_dataset.m which is
% in cts as a function of hz to horizontal displacement as a function
of hz.
% The need is fulfilled by the constant seism_dc which transforms
counts to
% horizontal acceleration. Then the ground is assumed to be a simple
harmonic
% oscillator such that (displacement) = (acceleration / (omega^2)).

if (~strcmp(IFO_NAME, 'C1'))
    seism_dc = 4e-7; % calibration of accelerometers in m*cts/s^2.

    seism = seism(2:end,:);
    seisv = seisv(2:end,:);

    %Horizontal Direction
    tmp = seism_dc ./ seism(:,1).^2;
    tt1 = tmp(cumsum(ones(length(tmp),5),1));
    tt1(:,1) = 1;
    seism = seism .* tt1;

    % Vertical Direction
    tmp = seism_dc ./ seisv(:,1).^2;
    tt2 = tmp(cumsum(ones(length(tmp),5),1));
    tt2(:,1) = 1;
    seisv = seisv .* tt2;

    seismos = SeismicNoise(seism(2:end,:),seisv(2:end,:));
elseif (strcmp(IFO_NAME, 'C1'))
    % The calibration constant seism_dc assumes the following:
    % 1) The Wilcoxon accelerometers are set to measure acceleration

```

Figure 7: Revised getSeismic.m Function Page 2

```

(cand not
%   velocity). The gain is 10 so that the conversion factor for
%   accelerometer output is 100 V/g
% 2) The ADC (analog to digital converter has range of (-2 V, 2 V)
%   and 16 bit resolution yielding a conversion factor from the
%   DAC input of 61.045 microV/count.
% 3) The ground may be approximated accurately as a simple harmonic
%   oscillator so that (displacement) = acceleration / (omega^2)

seism_dc = 5.9824e-06; % calibration of accelerometers m*cts/s^2

seism = seism(2:end,:);
seisv = seisv(2:end,:);

%Horizontal Direction
tmp = seism_dc ./ seism(:,1).^2;
tt1 = tmp(cumsum(ones(length(tmp),5),1));
tt1(:,1) = 1;
seism = seism .* tt1;

% Vertical Direction
tmp = seism_dc ./ seisv(:,1).^2;
tt2 = tmp(cumsum(ones(length(tmp),3),1));
tt2(:,1) = 1;
seisv = seisv .* tt2;

seismos = SeismicNoise40(seism(2:end,:), seisv(2:end,:));
end

```

Figure 8: Revised getSeismic.m Function Page 3

```

function [seismo] = SeismicNoise40(varargin)

% Author: unknown
%
% This 40 m specific function is part of the NB suite. The
% function takes as input the spectrum of ground acceleration
% at each test mass chamber in horizontal displacement as a function
% of hz and transforms that data into optical motion.
%
% This is done by first applying an accelerometer TF to transform
% the horizontal displacement as a function of hz read at the ADC to
% the actual horizontal displacement as a function of hz. Then a stack
% TF is applied to transform horizontal displacement at ground level
% as a function of hz to horizontal displacement on the stack as a
% function of hz. Finally a pendulum TF is applied to transform
horizontal
% displacement on the stack as a function of hz to optical displacement
% from equilibrium as a function of hz.
%
% Concerns:
% 1) Currently, the function is DARM specific. SeismicNoise.m also
%   calculates seismic noise contribution to MICH. Furthermore
%   SeismicNoise.m includes coupling between vertical and horizontal
%   motion due to the wedges (among other things). M. Jones 07/25/08
%
% 2) Currently, there is no vertical stack TF for the 40m. M. Jones
%   07/25/08
%
% 3) horizontal_adc is not the best possible estimate of the horizontal
%   noise (pre-accelerometer transfer function adjustment). A better
%   estimate should be obtained when the accelerometers are placed in
%   a final configuration. M. Jones 07/25/08.
%
% Revisions:
% 1) Revised from previous version to use accelerometer TF. M. Jones
%   07/25/08
%
%
global IFO_NAME FOTON_dir NB_DIR DARM_UGF DATA_dir UTIL_DIR coupldir
...
    NDS_HOST NDS_CHANNELS;

if nargin < 2
    error('Not enough Input Arguments')
elseif nargin < 4
    seism = varargin{1};

```

Figure 9: Revised SeismicNoise40.m Function Page 1

```

    seisv = varargin{2};
    loopname = 'DARM';

    if nargin > 2
        loopname = varargin{3};
    end
elseif nargin > 3
    error('Too Many Input Arguments')
end

% ===== Accelerometer Transfer Function =====
% The format of the file accelTF.txt is as follows:
% | f | M | p |
% | r | a | h |
% | e | g | a |
% | q | . | s |
% | . | . | e |
% | . | . | . |
% where phase is in degrees and magnitude is in decibels.

% Loading TF file
tmp = load('Data/accelTF40m.txt');

afreq = tmp(:,1);
amag = tmp(:,2);
%amag = 10 .^ (tmp(:, 2) ./ 20); % magnitude originally in dB
aphase = tmp(:,3);
clear tmp;

% Creating complex object
aG = amag .* exp(i * aphase * pi / 180 );

% ===== Stack Transfer Function =====
% The format of the stackTF40m.txt is as follows:
% | f | M | p |
% | r | a | h |
% | e | g | a |
% | q | . | s |
% | . | . | e |
% | . | . | . |
% where phase is in degrees and magnitude is in decibels.

% Loading TF file
tmp = load('Data/stackTF40m.txt');

```

Figure 10: Revised SeismicNoise40.m Function Page 2

```

sfreq = tmp(:,1);
smag = tmp(:,2);
%smag = 10 .^ (tmp(:, 2) ./ 20); % magnitude originally in dB
sphase = tmp(:,3);
clear tmp;

% Creating complex object
sG = smag .* exp(i * sphase * pi / 180);

% ===== Pendulum Transfer Function =====
% The format of the pendsTF40m.txt is as follows:
% | f | M | p |
% | r | a | h |
% | e | l | g | a |
% | q | . | l | s |
% | . | . | l | e |
% | . | . | l | . |
% where phase is in degrees and magnitude is in decibels.

% Loading TF file
tmp = load('Data/stackTF40m.txt');

pfreq = tmp(:,1);
pmag = tmp(:,2);
%pmag = 10 .^ (tmp(:, 2) ./ 20); % magnitude originally in dB
pphase = tmp(:,3);
clear tmp;

% Creating complex object
pG = pmag .* exp(i * pphase * pi / 180);

% ===== Generating Seismic Noise =====
% In this section the interp1 function is used to determine the
% magnitude of the transfer functions at the frequencies in the
% seismic fourier transform (f_adc). We then multiply these values
% by horizontal_adc (a rough estimate of the horizontal noise in m)
% to obtain horizontal_pend (an estimate of the pendulum displacement
% due
% to seismic noise). It is the mangnitude of horizontal_pend as a
% function
% of frequency which we use to estimate the seismic contribution to
% the
% noise budget.

f_adc = seism(:,1);

```

Figure 11: Revised SeismicNoise40.m Function Page 3

```

horizontal_adc = sqrt(seism(:,2).^2 + seism(:,3).^2 + seism(:,4).^2 +
seism(:,5).^2);

TF1 = interp1(afreq, aG, f_adc, 'spline','extrap');
TF2 = interp1(sfreq, sG, f_adc, 'spline','extrap');
TF3 = interp1(pfreq, pG, f_adc, 'spline','extrap');

horizontal_gnd = abs(TF1) .* horizontal_adc;
horizontal_stk = abs(TF2) .* horizontal_gnd;
horizontal_pend = abs(TF3) .* horizontal_stk;

% ===== Output =====

switch upper(loopname)
    case 'DARM'
        horizontal_noise = sqrt(horizontal_pend .^ 2);
    otherwise
        error('Invalid Loop Name');
end

if nargin == 1
    ]
    seismo = [f_adc horizontal_noise];
else
end

```

Figure 12: Revised SeismicNoise40.m Function Page 4